# Supporting Information for "Nanophotonic Heterostructures for Efficient Propulsion and Radiative Cooling of Relativistic Light Sails"

Ognjen Ilic, Cora M. Went, and Harry A. Atwater*
Thomas J. Watson Laboratories of Applied Physics
California Institute of Technology
Pasadena, CA 91125

*haa@caltech.edu

**SECTION 1: Parameters for analyzed heterostructures**

**Table S1.** Designed thin-film structures analyzed in this work. Reflectance $\langle \boldsymbol{R} \rangle$ corresponds to the averaged value in the $[\lambda_0, \lambda_f]$ interval (where $\lambda_0 = 1.2$ μm and $\lambda_f = 1.225\lambda_0$, corresponding to the Doppler-shifted laser wavelength at $\beta = 0.2$). Note the thinnest allowed layer in our analysis is 5 nm. The refractive index of the gap layer is $n_{\text{gap}} = 1$.

| Label | Layout: Material(Thickness [nm]) | $\boldsymbol{\rho_S}$ [g/m$^2$] | $\langle \boldsymbol{R} \rangle$ | $\boldsymbol{W}$ [$\sqrt{\text{g}}$/m] |
|---|---|---|---|---|
| A1 | $SiO_2$(206) | 0.453 | 0.12 | 0.151 |
| A3 | $SiO_2$(197) – gap(399) – $SiO_2$(197) | 0.867 | 0.37 | 0.068 |
| A5 | $SiO_2$(180) – gap(421) – $SiO_2$(182) – gap(421) – $SiO_2$(180) | 1.19 | 0.58 | 0.050 |
| A7 | $SiO_2$(156) – gap(452) – $SiO_2$(161) – gap(448) – $SiO_2$(161) – gap(452) – $SiO_2$(156) | 1.39 | 0.70 | 0.045 |
| A9 | $SiO_2$(130) – gap(484) – $SiO_2$(140) – gap(473) – $SiO_2$(143) – gap(473) – $SiO_2$(140) – gap(484) – $SiO_2$(130) | 1.51 | 0.76 | 0.043 |
| A11 | $SiO_2$(104) – gap(514) – $SiO_2$(124) – gap(492) – $SiO_2$(131) – gap(486) – $SiO_2$(131) – gap(492) – $SiO_2$(124) – gap(514) – $SiO_2$(104) | 1.58 | 0.78 | 0.0421 |
| B2 | Si(61) – $SiO_2$(5) | 0.154 | 0.65 | 0.0167 |
| B2’ | Si(54) – $SiO_2$(63) | 0.264 | 0.62 | 0.0230 |
| B3 | Si(61) – gap(550) – $SiO_2$(5) | 0.154 | 0.65 | 0.0165 |
| B3’ | Si(51) – gap(619) – $SiO_2$(73) | 0.279 | 0.64 | 0.0224 |
| B4 | Si(34) – gap(506) – Si(33) – $SiO_2$(5) | 0.166 | 0.82 | 0.0136 |
| B4’ | Si(33) – gap(523) – Si(31) – $SiO_2$(6) | 0.162 | 0.81 | 0.0137 |
| B4’’ | Si(5) – gap(631) – Si(45) – $SiO_2$(65) | 0.258 | 0.61 | 0.0224 |

**SECTION 2: Expressions for propulsion and radiative cooling of a laser-driven lightsail**

From Eq. (10) in [12], we have $\dot{\beta} = \frac{2P}{mc^2\gamma^3}\left(\frac{1-\beta}{1+\beta}\right)$, where $m$ is the total mass of the spacecraft (sail + payload). Since $\dot{\beta} = \frac{d\beta}{dL}\frac{dL}{dt} = \frac{d\beta}{dL}c\beta$, we have $\frac{dL}{d\beta} = \frac{mc^3\gamma^3\beta}{2P}\left(\frac{1+\beta}{1-\beta}\right)$. Substituting $P = R(\beta)P_0$ and $\gamma^2 = (1-\beta^2)^{-1}$ into the previous expression, we arrive at the equation (1) of the main text.

We write the absorbed power by the sail (Eq. 4) as $P_{\text{abs}}(\boldsymbol{x}, \beta) = P_0(\beta)A(\boldsymbol{x}, \beta)$, where $P_0(\beta)A(\boldsymbol{x}, \beta) = P_0(1-\beta)/(1+\beta)a(\boldsymbol{x}, \beta)$ accounts for the Doppler-shift of the laser photon flux as seen by the sail[1], and $a(\boldsymbol{x}, \beta)$ is the absorptivity of the sail. The blackbody spectral intensity is given by $I_{\lambda b}(T) = \frac{2hc^2}{\lambda^5}\frac{1}{\text{Exp}\left[\frac{hc}{\lambda k_B T}\right]-1}$. The hemispherical-spectral (hs) emissivity $\epsilon_\lambda(\boldsymbol{x}, T)$ in Eq. (5) of the main text is the sum of the front and the back surface (hs) emissivities, namely

$$\epsilon_\lambda(\boldsymbol{x}, T) = \epsilon_\lambda^F(\boldsymbol{x}, T) + \epsilon_\lambda^B(\boldsymbol{x}, T) \tag{S1}$$

where the hemispherical-spectral emissivity is related to the directional-spectral emissivity as

$$\epsilon_\lambda^F(\boldsymbol{x}) = \frac{1}{\pi}\iint \epsilon_\lambda^F(\boldsymbol{x},\theta,\phi)\cos\theta\sin\theta\, d\theta d\phi \tag{S2}$$

and, from Kirchhoff's law, $\epsilon_\lambda^F(\boldsymbol{x},\theta,\phi) = a_\lambda^F(\boldsymbol{x},\theta,\phi) = 1 - R_\lambda^F(\boldsymbol{x},\theta,\phi) - T_\lambda^F(\boldsymbol{x},\theta,\phi)$, where $R, T$ denote the reflectivity and transmissivity coefficients. Finally, we can relate the front and the back surface emissivities as $\epsilon_\lambda^F(\boldsymbol{x}) = \epsilon_\lambda^B(-\boldsymbol{x})$.

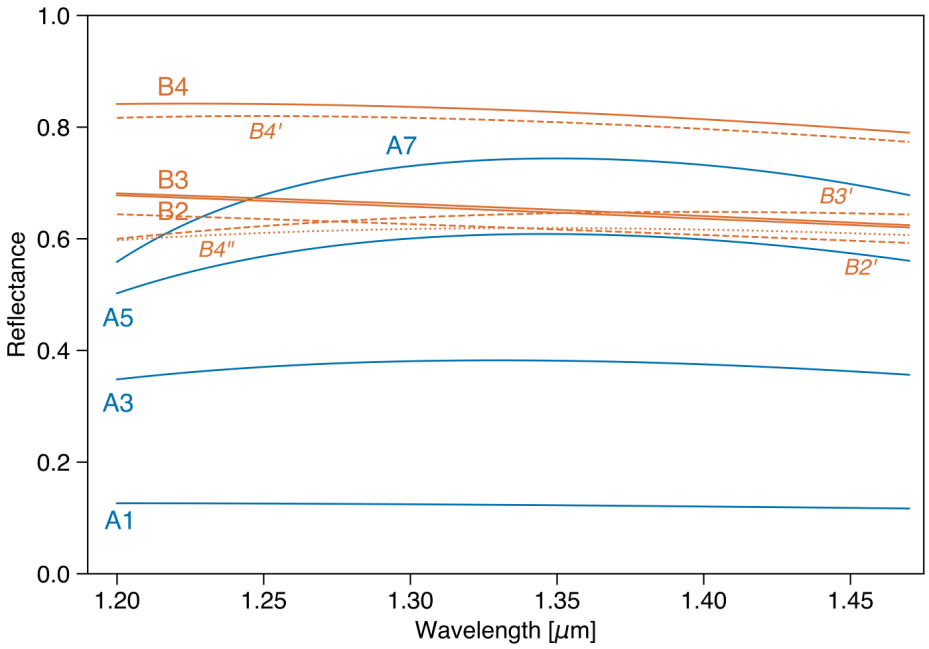


***Fig S1.*** Spectral reflectance (at normal incidence) in the laser propulsion band for the structures from Table S1.

**SECTION 3: Sensitivity of figure of merit to $n > 1$ gap refractive index**

For multilayer silica structures from Fig. 3, we assume vacuum gap(s) with refractive index of unity. Instead of vacuum, one could envision gaps formed by low-absorption, low-density aerogel materials with $n > 1$ refractive indices [25-28]. To characterize the RAAD sensitivity to greater-than-unity refractive index, we perform the same optimization analysis for silica structures (Fig. 3), but with $n_{\text{gap}} = 1.1$ (and $\rho_{\text{gap}} \sim 0.1\ \text{g cm}^{-3}$, to model aerogel density)[2]. The result is shown in Fig. S2, and the corresponding structure parameter listed in Table S2. We note approximately 25-30% increase in $W$ relative to the case of unity gap refractive index.

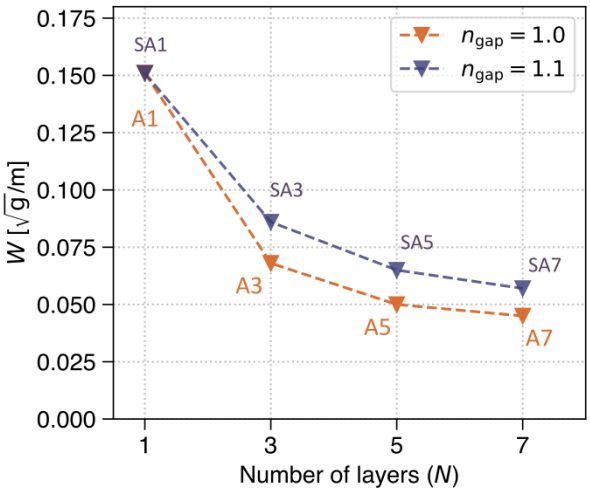


***Fig. S2.*** Comparison of designed silica multilayer stacks with different gap layer refractive index. Stack parameters are listed in Tables S1 & S2.

**Table S2.** Designed thin-film $SiO_2$ structures when the refractive index of the gap layer is $n_{gap} = 1.10$. The rest of the parameters are the same as in Table S1.

| Label | Layout: Material(Thickness [nm]) | $\boldsymbol{\rho_S}$ [g/m$^2$] | $\langle \boldsymbol{R} \rangle$ | $\boldsymbol{W}$ [$\sqrt{\text{g}}$/m] |
|---|---|---|---|---|
| SA1 | $SiO_2$(206) | 0.453 | 0.12 | 0.151 |
| SA3 | $SiO_2$(203) – gap(361) – $SiO_2$(203) | 0.929 | 0.30 | 0.086 |
| SA5 | $SiO_2$(196) – gap(369) – $SiO_2$(193) – gap(369) – $SiO_2$(196) | 1.36 | 0.47 | 0.065 |
| SA7 | $SiO_2$(186) – gap(382) – $SiO_2$(184) – gap(379) – $SiO_2$(184) – gap(382) – $SiO_2$(186) | 1.74 | 0.61 | 0.057 |

## SECTION 4: Infrared extinction coefficients of silica & silicon

In contrast to vibrational modes in silica, the fundamental vibration in undoped silicon has no dipole moment due to crystal symmetry and is therefore infrared inactive. The interaction of phonons with light can occur via higher order atomic displacements. Consequently, the measured extinction coefficient of undoped silicon (resistivity $> 10^3$ Ω cm) in the mid infrared is orders of magnitude smaller than that of silica (Fig. S3).

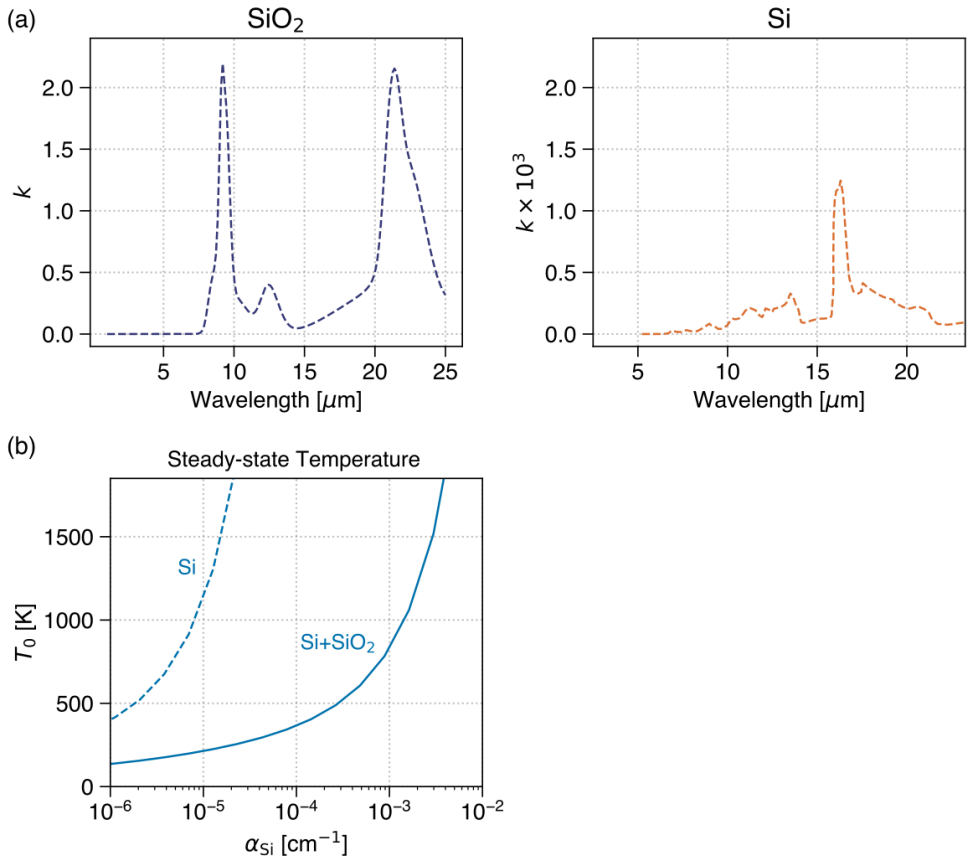


***Fig S3.*** (a) Comparison of mid-IR extinction coefficients for silica (Kitamura et al. [18]) and undoped silicon (Chandler-Horowitz & Amirtharaj [21]). For silicon, $k$ is multiplied by $10^3$. (b) Steady-state temperature for the B2 stack (Si + 5nm of $SiO_2$, solid line) and the same stack without $SiO_2$ (dashed line). The 5nm $SiO_2$ film increases $W$ only marginally (~3%), but can enable significantly lower steady-state temperatures. Here, we assume $P_0/m_p = 100$ GW g$^{-1}$, and $\alpha_{SiO_2} = 10^{-6}$ cm$^{-1}$.

**References**


1. Landau, L. D. & Lifshitz, E. M. *The Classical Theory of Fields (Fourth Edition)* **2,** (Pergamon, 1975).
2. Bellunato, T., Calvi, M., Matteuzzi, C., Musy, M., Perego, D. & Storaci, B. Refractive index of silica aerogel: Uniformity and dispersion law. *Nucl. Instruments Methods Phys. Res. Sect. A Accel. Spectrometers, Detect. Assoc. Equip.* **595,** 183–186 (2008).